Chapter 4
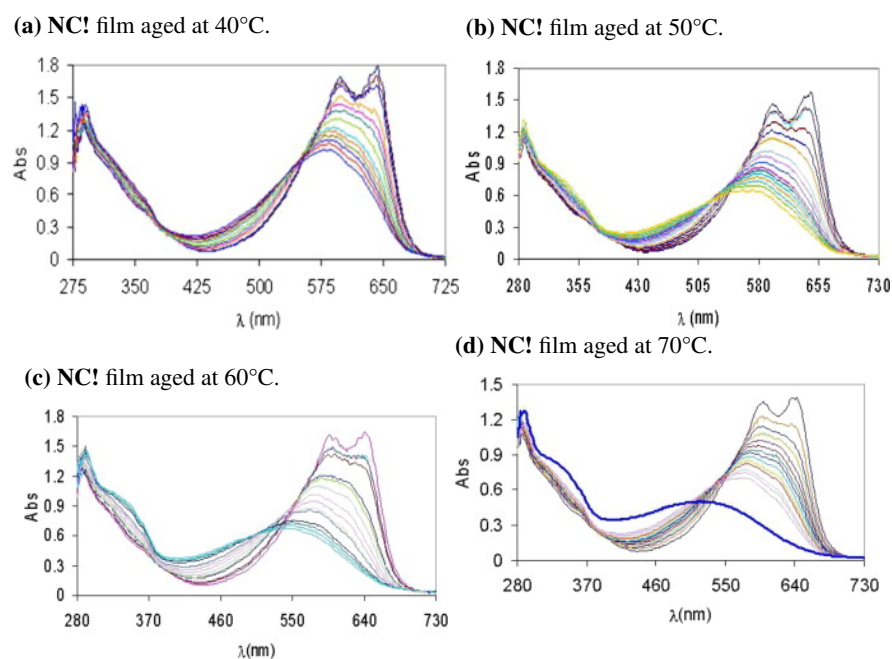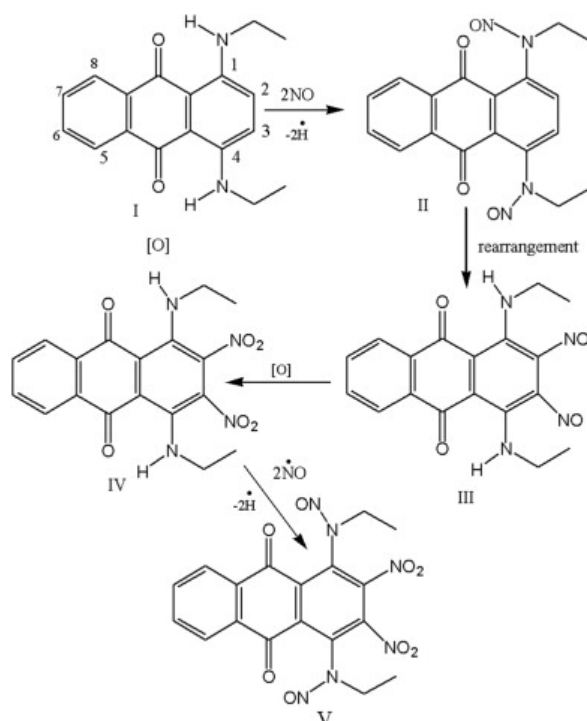
Post-Denitration Reactions

4.1   Introduction

Products of the preliminary denitration step of **NC!** (**NC!**) can be evolved as gases or remain trapped in the polymer matrix. Reactive nitrous oxide radicals generated from homolysis of the O-N bond are likely to migrate within the bulk and attack other sites on the polysaccharide. Nitrous and nitric acids released directly from denitration, or via transformation of released NO_x species, contribute to the acidity of the overall system, lowering the pH and stimulating further hydrolysis processes [**?**].

When studying the ageing of **NC!** using **UVVis!** spectroscopy, Moniruzzaman *et al.* observed increasing concentrations of secondary reaction products following heat treatment over extended timescales[**?**, **?**]. Samples exposed to higher ageing temperatures presented spectra dominated by consecutive products (figure 4.1). **UV!** absorbances at 600 nm and 650 nm were characteristic of the **SB59!** (**SB59!**) dye used to indicate the presence of NO_x, released by the denitration of **NC!**. The isosbestic point identified at 552 nm showed that as the concentration of **SB59!** decreased, the concentration of the [**SB59!** + **NC!**] product increased. For sample aged at temperatures >40°C, the isosbestic point demostrated a downwards shift. In the case of the 70°C treated run, the final measurement (indicated by the royal-blue line in bold, figure 4.1d) deviated from the isosbestic point entriely, and showed more than 81% consumption of the original dye concentration. The drift from the isosbestic point, in addition to the appearance of new absorabce peaks below 400 nm, alludes to the presence of new species in the reaction mixture not generated by the primary reaction of **SB59!** and **NC!**. It is likely that these arise from the continued reaction of **SB59!** derivatives with **NC!** degradation products, or further derivatives thereof, as suggested in scheme 4.1.

(a) NC! film aged at 40°C.

(b) NC! film aged at 50°C.

(d) NC! film aged at 70°C.

(c) NC! film aged at 60°C.

Figure 4.1: UVVis! spectra of aged **NC!**-based film, from the work of Moniruzzaman *et al.*[**?**]. The peaks at 600 nm and 650 nm are attributed to the π - π* transitions in the anthraquinone dye (**SB59!**). Spectral lines with highest absorbance peaks in this region correspond to the [**NC! + SB59!**] sample prior to heat treatment. Peaks below 400 nm indicate the formation of **SB59!** derivatives due to secondary reactions.
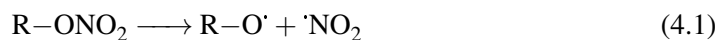

Scheme 4.1: Proposed pathway for the reaction of **SB59!** dye with ·NO released as a result of denitration of **NC!** [**?**].
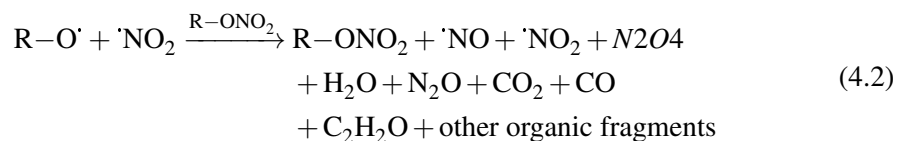
Following cleavage of the nitrate ester via homolytic fission, elimination of nitrous acid, or hydrolysis, the resulting residues are available for further reaction with the polymer or other free molecules in the system. Chin *et al.* proposed schemes for the propagation of such reactions initated by both the thermolysis and hydrolysis of nitrate esters [**?**] :
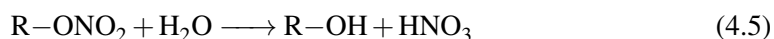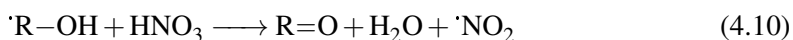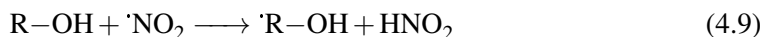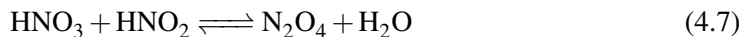
Thermolysis
Initiation:

$$R-ONO_2 \longrightarrow R-O^{\cdot} + {}^{\cdot}NO_2 \tag{4.1}$$

Propagation:

$$R-O^{\cdot} + {}^{\cdot}NO_2 \xrightarrow{R-ONO_2} R-ONO_2 + {}^{\cdot}NO + {}^{\cdot}NO_2 + N2O4$$
$$+ H_2O + N_2O + CO_2 + CO$$
$$+ C_2H_2O + \text{other organic fragments} \tag{4.2}$$

$$2\,{}^{\cdot}NO + O_2 \longrightarrow 2\,{}^{\cdot}NO_2 \tag{4.3}$$

$$2\,{}^{\cdot}NO_2 \rightleftharpoons N_2O_4 \tag{4.4}$$

Hydrolysis
Initiation:

$$R-ONO_2 + H_2O \longrightarrow R-OH + HNO_3 \tag{4.5}$$

$$R-OH + HNO_3 \longrightarrow R{=}O + HNO_2 + H_2O \tag{4.6}$$

Propagation:

$$HNO_3 + HNO_2 \rightleftharpoons N_2O_4 + H_2O \tag{4.7}$$

$$N_2O_4 \rightleftharpoons 2\,{}^{\cdot}NO_2 \tag{4.8}$$

$$R-OH + {}^{\cdot}NO_2 \longrightarrow {}^{\cdot}R-OH + HNO_2 \tag{4.9}$$

$${}^{\cdot}R-OH + HNO_3 \longrightarrow R{=}O + H_2O + {}^{\cdot}NO_2 \tag{4.10}$$
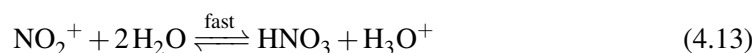
The hydrolysis scheme was adapted from an earlier work by Camera *et al.* involving the nitrate ester decomposition and subsequent reactions of ethyl nitrate (where R = CH_3CH_2 for the scheme above) [**?**]. The original study included the expansion of the hydrolysis step (equation $PhCH_2ONO_2$,), where the involvement of NO_2^+ can be seen:

Hydrolysis

$$CH_3CH_2ONO_2 + H^+ \xrightleftharpoons{fast} CH_3CH_2ONO_2H^+ \tag{4.11}$$

$$CH_3CH_2ONO_2H^+ \xrightleftharpoons{slow} CH_3CH_2H + NO_2^+ \tag{4.12}$$

$$NO_2^+ + 2\,H_2O \xrightleftharpoons{fast} HNO_3 + H_3O^+ \tag{4.13}$$
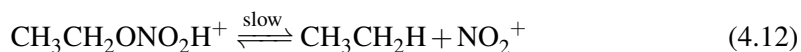
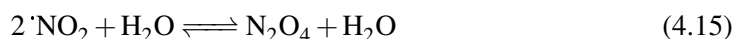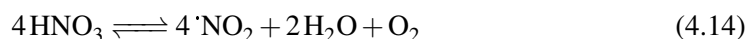It was highlighted by Camera, that the oxidation of alchol by nitric acid (equation 4.6) is slow and thus rate-limiting. The mechanism is likely to occur *via* a series of intermediate reactions of which the details are not known. However, following the generation of nitrous acid, subsequent oxidations occur rapidly. Equations 4.7 - 4.10 describe a possible branched radical chain mechanism, fed by the nitrous and nitric acids produced during the hydrolysis and alchohol oxidation reactions during the initiation stages.
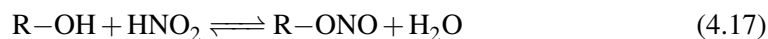
By contrast, the propagation reactions in the branched radical chain mechanism for thermolysis are poorly characterised (equation 4.2), defined only by the observable products. This is likely due to their rapid and varied nature, rendering it difficult to follow spectroscopically. Termination reactions were not emphasised in the schemes, for these cases.

Aellig *et al.* presented an alternative scheme when determining the decomposition of benzyl nitrate (R = PhCH$_2$), involving more interaction with the solvent [**?**]:

Initiation

$$4\,HNO_3 \rightleftharpoons 4\,{}^{\bullet}NO_2 + 2\,H_2O + O_2 \tag{4.14}$$

$$2\,{}^{\bullet}NO_2 + H_2O \rightleftharpoons N_2O_4 + H_2O \tag{4.15}$$

$$N_2O_4 + H_2O \longrightarrow HNO_3 + HNO_2 \tag{4.16}$$

Propagation

$$R-OH + HNO_2 \rightleftharpoons R-ONO + H_2O \tag{4.17}$$

$$R-ONO \longrightarrow R{=}O + HNO \tag{4.18}$$

$${}^{\bullet}NO_2 + HNO \longrightarrow HNO_2 + {}^{\bullet}NO \tag{4.19}$$

$$2\,{}^{\bullet}NO + O_2 \longrightarrow 2\,{}^{\bullet}NO_2 \tag{4.20}$$

Termination

$$2\,HNO \longrightarrow HON{=}NOH \tag{4.21}$$

$$HON{=}NOH \longrightarrow N_2O + H_2O \tag{4.22}$$
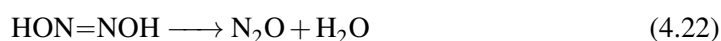
However, for the initiation reactions Aellig prescribes the use of an amberlyst catalyst, The propagation reactions are acid catalysed by HNO$_2$.

Both the Camera/Chin and Aellig schemes above produce final end products observed in the decomposition of **NC!**. In particular, Aeelig's scheme accounts for the production of N$_2$O, which forms a XXXX part of the decomposition eluent.

It is widely agreed that first-stage decomposition follows a first-order process (or pseudo-first order, with respect to hydrolysis reactions). A number of studies observe cat-

alytic rate of decay for the longer-term aging processes. Dauerman [**?**] observed that when **NC!** was treated with NO_2 gas before heating, the time required for sample ignition halved. He suggested that the NO_2 adsorbed onto the surface acted as a catalysing agent.

Neutral and alkaline hydrolysis reactions follow a pseudo-first order process, however it has been suggested that the presence of acid facilitiatles a catalyic rate of degradation after an initial incubation period.

Multiple studies have addressed the decomposition reactions of nitrate esters following the initial scission of the nitrate group [**?, ?, ?, ?, ?, ?**]

In this section, secondary and extended reaction schemes for the low temperature ageing of **NC!** are explored. Decompostition pathways defined by Camera *et al.* and Aellig *et al.* are probed to determine the reactions responsible for the experimentally observed degradation products. The reactions found to be energetically feasible from the proposed routes will be scrutinised to determine whether an autocatalytic pathway can be formed from the energitcally validated reaction schemes.

4.2   Methodology

The equations proposed by Chin, Camera and Aellig *et al.* were applied to the degradation of **NC!**. The products of homolytic fission, intramolecular elimination of HNO_2 and acid hydrolysis as the starting point for forward propagation of

Schemes 4.2 - 4.4 were constructed based on the step-wise progression of each stage of decomposition

The species reactions were geometry optimised using **wb97xd!** (**wb97xd!**), and **B3LYP!** (**B3LYP!**) functionals, in both vacuum and solvent. The reactions were modelled using ethyl nitrate as a test system before expansion to the full C2 monomeric model. The **DG!** (**DG!**) were used to determine the feasibility of a reaction. Where the choice of method lead to a variation in the result

4.2.1   Computational details

All geometry optimisations were performed in **G09!** (**G09!**), using the **wb97xd!** and **B3LYP!** functionals. Optimisations were repeated with **PCM!** (**PCM!**) to introduce solvent effects.

4.3 Results and Discussion

4.3.1 Thermodynamics of Ethyl Nitrate reactions

The reaction energies for the proposed schemes

Table 4.1: Free energies of protonation for each oxygen site on ethyl nitrate.

Protonated site		ΔG_r /kcal mol^{-1}			
		wb97xd!	PCM	**B3LYP!**	PCM
Terminal (up)	$CH_3CH_3ONO_2H^+$	-12.2768	8.8219	-13.7825	5.6253
Terminal (down)	$CH_3CH_3ONO_2H^+$	-9.4752	9.4595	-11.1321	5.6461
Bridging	$CH_3CH_3O(H^+)NO_2$	-9.3227	9.0581	-15.3096	6.6736

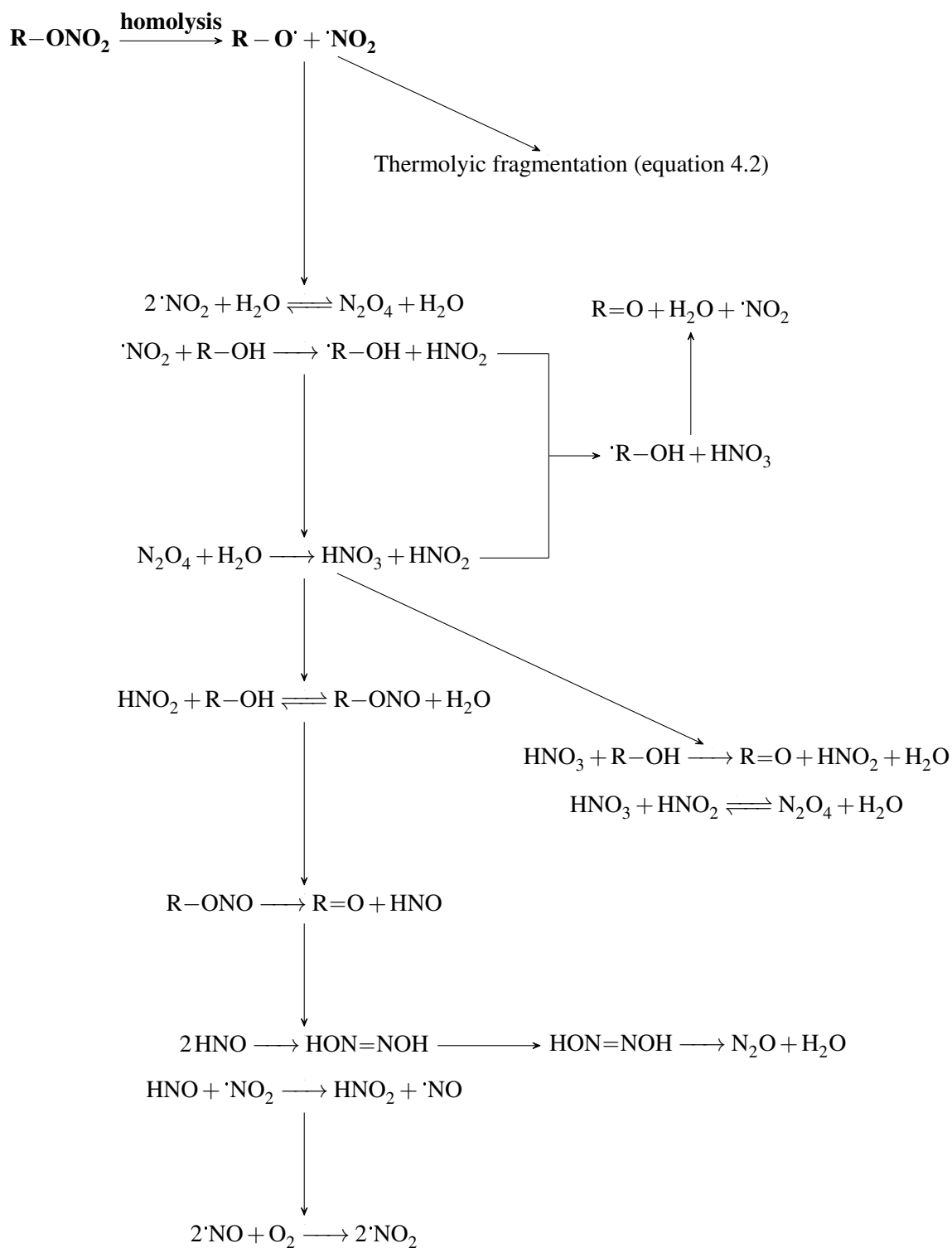**(a)** Upper terminal oxgen.   **(b)** Lower terminal oxgen.   **(c)** Bridging oxgen.
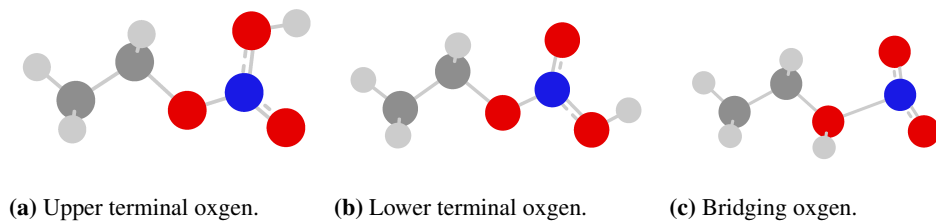
Figure 4.2: Possible sites of protonation on ethyl nitrate.

Collation of the above schemes to fit the starting products from denitration:

Insights into the reaction energies "HNO cannot be stored or concentrated and is typically studied using donor species that release HNO as a decomposition product." (paper since retracted)

4.4 Summary

$$\mathbf{R{-}ONO_2} \xrightarrow{\textbf{homolysis}} \mathbf{R - O^{\cdot} + {}^{\cdot}NO_2}$$

Thermolyic fragmentation (equation 4.2)

$$2\,{}^{\cdot}NO_2 + H_2O \rightleftharpoons N_2O_4 + H_2O$$

$$R{=}O + H_2O + {}^{\cdot}NO_2$$

$${}^{\cdot}NO_2 + R{-}OH \longrightarrow {}^{\cdot}R{-}OH + HNO_2$$

$${}^{\cdot}R{-}OH + HNO_3$$

$$N_2O_4 + H_2O \longrightarrow HNO_3 + HNO_2$$

$$HNO_2 + R{-}OH \rightleftharpoons R{-}ONO + H_2O$$

$$HNO_3 + R{-}OH \longrightarrow R{=}O + HNO_2 + H_2O$$

$$HNO_3 + HNO_2 \rightleftharpoons N_2O_4 + H_2O$$

$$R{-}ONO \longrightarrow R{=}O + HNO$$

$$2\,HNO \longrightarrow HON{=}NOH \longrightarrow HON{=}NOH \longrightarrow N_2O + H_2O$$

$$HNO + {}^{\cdot}NO_2 \longrightarrow HNO_2 + {}^{\cdot}NO$$

$$2\,{}^{\cdot}NO + O_2 \longrightarrow 2\,{}^{\cdot}NO_2$$

Scheme 4.2: Proposed degradation pathway starting from the homolysis products of a nitrate ester, derived from the schemes presented by Camera [**?**] and Aellig[**?**].

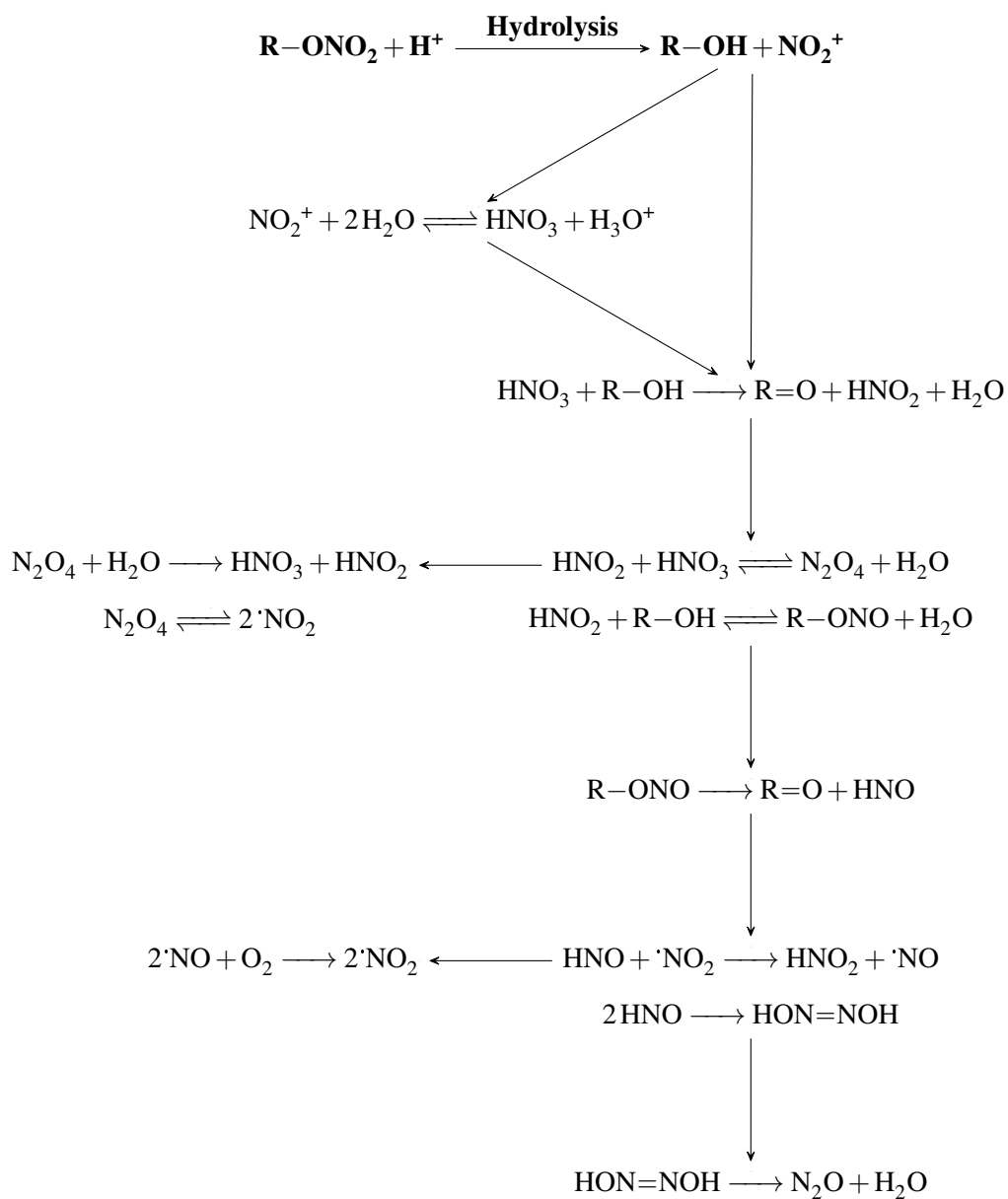$$\textbf{R}-\textbf{ONO}_\textbf{2} \xrightarrow{\textbf{Elimination}} \textbf{R}=\textbf{O} + \textbf{HNO}_\textbf{2}$$

$$HNO_2 + R-OH \rightleftharpoons R-ONO + H_2O$$

$$R-ONO \longrightarrow R=O + HNO$$

$$2\,HNO \longrightarrow HON=NOH$$

$$HNO + \dot{N}O_2 \longrightarrow HNO_2 + \dot{N}O$$

$$HON=NOH \longrightarrow N_2O + H_2O$$
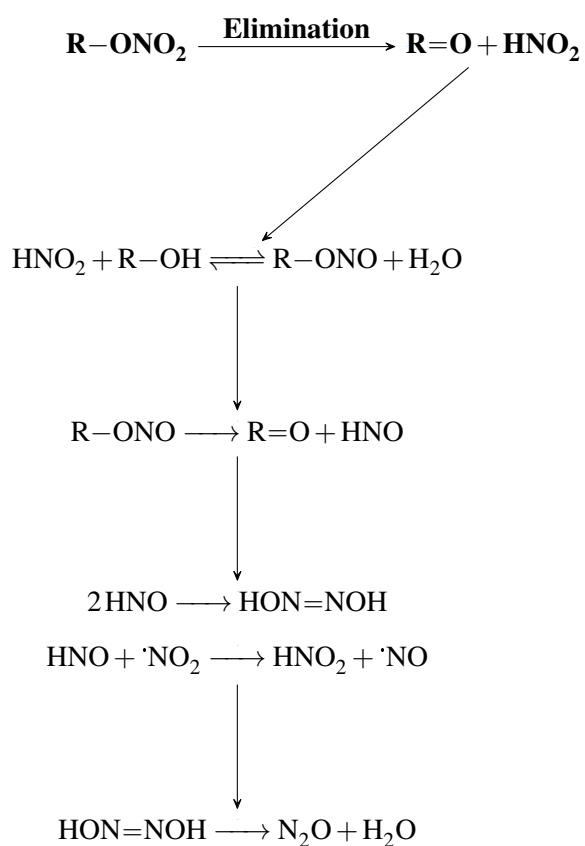
Scheme 4.3: Proposed degradation pathway starting from the elimination of HNO_2 from a nitrate ester, derived from the schemes presented by Camera [?] and Aellig[?].

$$\textbf{R}-\textbf{ONO}_2 + \textbf{H}^+ \xrightarrow{\textbf{Hydrolysis}} \textbf{R}-\textbf{OH} + \textbf{NO}_2^+$$

$$NO_2^+ + 2\,H_2O \rightleftharpoons HNO_3 + H_3O^+$$

$$HNO_3 + R-OH \longrightarrow R{=}O + HNO_2 + H_2O$$

$$N_2O_4 + H_2O \longrightarrow HNO_3 + HNO_2 \longleftarrow HNO_2 + HNO_3 \rightleftharpoons N_2O_4 + H_2O$$

$$N_2O_4 \rightleftharpoons 2\,{}^{\bullet}NO_2 \qquad\qquad HNO_2 + R-OH \rightleftharpoons R-ONO + H_2O$$

$$R-ONO \longrightarrow R{=}O + HNO$$

$$2\,{}^{\bullet}NO + O_2 \longrightarrow 2\,{}^{\bullet}NO_2 \longleftarrow HNO + {}^{\bullet}NO_2 \longrightarrow HNO_2 + {}^{\bullet}NO$$

$$2\,HNO \longrightarrow HON{=}NOH$$

$$HON{=}NOH \longrightarrow N_2O + H_2O$$

Scheme 4.4: Proposed degradation pathway starting from the acid hydrolysis of a nitrate ester, derived from the schemes presented by Camera [**?**] and Aellig[**?**].

Table 4.2: Energies of nitrate ester decomposition reactions proposed by Camera [**?**], Chin [**?**] and Aellig [**?**]. R = CH_3CH_2 for ethyl nitrate, and R = $(H_3CO)_2C_6H_9O_3$ (bi-methoxy capped glucopyraonse monomer unit).

Reaction	ΔG_r /kcal mol^{-1}			
	wb97xd!	PCM	**B3LYP!**	PCM
$NO_2^+ + 2\,H_2O \rightleftharpoons HNO_3 + H_3O^+$	-0.8965	-1.3388	1.7703	2.4646
$2\,{}^{\cdot}NO + O_2 \longrightarrow 2\,{}^{\cdot}NO_2$	-20.7705	-21.9731	-21.1604	-22.1590
$2\,{}^{\cdot}NO_2 \rightleftharpoons N_2O_4$	-0.1222	-1.3104	0.5418	0.1556
$HNO_3 + HNO_2 \rightleftharpoons N_2O_4 + H_2O$	-2.2516	-1.8541	-5.1314	-4.1801
$N_2O_4 \rightleftharpoons 2\,{}^{\cdot}NO_2$	0.1235	1.4616	-0.5393	-0.1556
$4\,HNO_3 \rightleftharpoons 4\,NO_2 + 2\,H_2O + O_2$	53.3503	58.3645	42.6094	46.9356
$2\,{}^{\cdot}NO_2 + H_2O \rightleftharpoons N_2O_4 + H_2O$	-0.1222	-1.4616	0.5393	0.1556
$N_2O_4 + H_2O \longrightarrow HNO_3 + HNO_2$	2.2516	1.8541	5.1314	4.1801
${}^{\cdot}NO_2 + HNO \longrightarrow HNO_2 + {}^{\cdot}NO$	-28.2164	-28.6682	-27.3269	-27.6255
$2\,{}^{\cdot}NO + O_2 \longrightarrow 2\,{}^{\cdot}NO_2$	-59.8947	-60.4724	-60.4687	-60.9960
$2\,HNO \longrightarrow HON{=}NOH$	-38.9693	-39.7158	-36.6276	-37.4081
$HON{=}NOH \longrightarrow N_2O + H_2O$	-48.0829	-48.1843	-50.5531	-50.7490
Ethyl nitrate (R = CH_3CH_2)				
$R{-}OH + HNO_3 \longrightarrow R{=}O + HNO_2 + H_2O$	-34.0622	-38.4275	-37.5940	-41.7703
$R{-}OH + {}^{\cdot}NO_2 \longrightarrow {}^{\cdot}R{-}OH + HNO_2$	16.3762	13.9230	15.8873	13.6994
${}^{\cdot}R{-}OH + HNO_3 \longrightarrow R{=}O + H_2O + {}^{\cdot}NO_2$	-50.4384	-52.3505	-53.4813	-55.4715
$R{-}OH + HNO_2 \rightleftharpoons R{-}ONO + H_2O$	-3.2054	-3.2760	-2.6410	-2.9490
$R{-}ONO \longrightarrow R{=}O + HNO$	-1.4963	-5.8218	-4.3672	-8.5012
NC! monomer (R = $(H_3CO)_2C_6H_9O_3$)				
$R{-}ONO_2 + H_2O \longrightarrow R{-}OH + HNO_3$	0.6754	5.6309	0.6124	-0.7012
$R{-}OH + {}^{\cdot}NO_2 \longrightarrow {}^{\cdot}R{-}OH + HNO_2$	14.7130	11.1516	13.0341	23.2098
${}^{\cdot}R{-}OH + HNO_3 \longrightarrow R{=}O + H_2O + {}^{\cdot}NO_2$	-51.4382	-49.4947	-54.7483	-56.3693
$R{-}OH + HNO_2 \rightleftharpoons R{-}ONO + H_2O$	-4.4314	-7.3023	-4.3061	-0.1783
$R{-}ONO \longrightarrow R{=}O + HNO$	-2.9333	-1.7111	-6.8223	-11.2058